Cement and Concrete Composites 148 (2024) 105484

Contents lists available at ScienceDirect

Cement and Concrete Composites

journal homepage: www.elsevier.com/locate/cemconcomp

The secret of ancient Roman hydraulic mortar: the lesson learnt from the past for future cements

Laura Medeghini [a,b,*], Laura Calzolari [a], Michela Botticelli [c], Melania Di Fazio [a], Caterina De Vito [a], Ida Pettiti [d], Fabrizio Bardelli [e], Silvano Mignardi [a]

[a] Department of Earth Sciences, Sapienza University of Rome, Piazzale A. Moro, 5, 00185, Rome, Italy
[b] CNIS, Sapienza University of Rome, Piazzale A. Moro, 5, 00185, Rome, Italy
[c] Kelvin Centre for Conservation and Cultural Heritage Research, University of Glasgow, Kelvin Hall, 1445 Argyle Street, Glasgow, G3 8AW, UK
[d] Department of Chemistry, Sapienza University of Rome, Piazzale Aldo Moro, 5, 00185, Rome, Italy
[e] CNR-Nanotec, Institute of Nanotechnology, Piazzale Aldo Moro, 5, 00185, Rome, Italy

ARTICLE INFO

Keywords:
Amorphous material
C-A-S-H
C-(N,K)-A-S-H
Pozzolan
Mortar
Microstructure

ABSTRACT

Aqua Traiana is an ancient Roman aqueduct, built to supply water to the ancient city of Rome and still working nowadays. This work is focused on the characterization of its mortars, and in particular the binders, to identify the reasons of such a durable resistance. Samples collected inside the aqueduct were analysed by Optical Microscopy (OM) in thin sections, X-ray Powder Diffraction (XRPD), Scanning Electron Microscopy with Energy-Dispersive X-ray Spectroscopy (SEM-EDS), High Resolution Field Emission Scanning Electron Microscopy (HR-FESEM-EDS), Electron Microprobe (EMPA), Differential Scanning Calorimetry coupled with Thermogravimetric Analysis (DSC-TGA), Fourier-Transform Infrared spectroscopy (FTIR), X-ray Absorption Near Edge Structure (XANES) spectroscopy and N_2 adsorption/desorption measurements. The presence of an amorphous gel-like C-(N,K)-A-S-H binder and the complete absence of calcite in Trajan Age samples constitute a unique case, and may be the reason of the high hydraulicity of the mortar. Establishing how these features were produced could allow them to be replicated in high-durability and high-compatibility restoration mortars.

1. Introduction

Mortars and concretes are artificial materials produced by human beings since antiquity starting from natural materials. The first applications were mainly limestone or gypsum-based plasters starting from 9000 BCE. The ancient technology was based on burning limestone or gypsum, grinding the heated block, and slaking it with water. After the application, the paste reacted with the CO_2 in the atmosphere producing a hard and resistant material. During Roman times, lime plasters and mortars were more widespread, due to their higher strength and durability compared to gypsum [1]. An important improvement is represented by the mixing of slaked lime with high-alkali products and volcanic ash to produce hard, durable, and waterproof materials, both in terrestrial [2–4] and in marine environments [5,6]. The addition of pozzolanic material to the aerial lime was not a Roman discovery, although Romans were the first to use such mortars widely [7].

Roman hydraulic mortars are an example of high technological level of ancient civilizations, therefore their characterization has received great attention in archaeometric studies [2–5]. The mineralogy of the pozzolanic aggregate has been studied in detail [3,4,8–12], and it has been proved that ancient Romans considered the volcanic materials from Monti Sabatini, the Alban Hills, and Pozzuoli's surroundings as the best aggregates to manufacture good hydraulic mortars [8,10,13,14]. Nowadays, the pozzolanic aggregates added to Portland cements to improve their mechanical features are called Supplementary Cementitious Materials (SCMs) and includes fly ash and slag [7,15,16].

Despite the widespread interest in Roman hydraulic mortars [17], only few scientific studies have been conducted to investigate them in ancient Roman aqueducts [18–20], or in building materials used in the ancient aqueducts [21–23]. Concerning the city of Rome, few archaeometric studies were published so far on Roman aqueducts and on their building materials [24,25]. The methods usually applied in the archaeometric studies of ancient mortars include optical microscopy in thin sections (OM), X-ray powder diffraction (XRD), IR [26] and Raman [27] spectroscopy, Scanning Electron Microscopy (SEM-EDS) [3] thermogravimetric, mechanical [28], and porosimetric analysis [29].

* Corresponding author Department of Earth Sciences, Sapienza University of Rome, Piazzale A. Moro, 5, 00185, Rome, Italy.
E-mail address: laura.medeghini@uniroma1.it (L. Medeghini).

https://doi.org/10.1016/j.cemconcomp.2024.105484
Received 13 September 2023; Received in revised form 18 January 2024; Accepted 18 February 2024
Available online 20 February 2024

Recently the application of synchrotron radiation techniques has given a major boost to this field [30,31].

The typical features of lime–pozzolan mortars, such as high strength, insolubility, and their ability to maintain their properties even under water, ensured their success in ancient times [12]. Pozzolan fragments are made of highly reactive aluminosilicates, with a high fraction of amorphous/glassy materials. These are mixed with calcium hydroxide, i.e. hydrated lime, according to the reaction:

(1) CaO (lime) + H_2O (water) → $Ca(OH)_2$

The pozzolanic materials consume the hydrated lime, as in (2), producing Calcium Silicate Hydrates C–S–H and Calcium Aluminosilicate Hydrates C-A-S-H, which confer hydraulicity to the mortar.

(2) $Ca(OH)_2$ + pozzolan (reactive silicates and aluminosilicates) + H_2O (water) → C-S–H ± C-A-S-H

The process results in the formation of reaction rims surrounding the aggregates [32].

In an effective pozzolanic system, $Ca(OH)_2$ should be fully consumed by the reaction (2). After time calcite can be formed by the carbonatation of the excess $Ca(OH)_2$, or by the degradation of C-S–H and C-A-S-H [17,33].

Among the Roman aqueducts, the *Aqua Traiana* aqueduct (Rome, 2nd century AD) represents a unique case study, because of its long history and extraordinary resistance to decay processes, which is mainly attributed to the high durability of its hydraulic mortars, still maintaining their function.

It was built by Emperor Trajan in 109 AD and carried water for 57 km from the springs located north of Lake Bracciano to *Trastevere* in the city of Rome, where water mills were located in ancient times [34,35]. After several destructions during the barbarian invasions, it was finally restored by pope Paulus V (1609–1612) [35,36], and it still carries water to Rome today.

Preliminary archaeometric analysis on both ancient mortars (those dated back to the Trajan Era and those belonging to the papal restoration) has indicated a unique composition of the mortars of the Trajan phase, which has never been observed before. As expected, in the Trajan and papal mortars, the aggregate was mainly composed of pyroclastic products with pozzolanic behaviour from the Roman Magmatic Province. On the contrary, the expected typical calcitic lime binder was observed only in the papal mortars. In addition, unlike the papal samples and the other Roman hydraulic mortars studied until now, the Trajan binder resulted calcite-free and amorphous [18–20].

In order to understand if such extraordinary resistance and durability are related to the original Trajan mortars, to those of papal restoration or both, a mineralogical, physical, microstructural, and chemical characterization of both mortar binders from the ancient *Aqua Traiana* was performed to help revealing the materials employed and the chemical reactions which occurred.

The results of this study are intended to offer a clearer historical and archaeological context. Moreover, modern applications may benefit from a better understanding of ancient mortar technology.

2. Materials and methods

2.1. Samples

Samples were collected inside a still functioning secondary duct at Sette Botti - Trevignano Romano, in the northern area of Lake Bracciano (Rome, Italy). Mortar samples were collected from areas identified by the archaeologists as belonging to the Trajan Age and to the papal restoration works, based on macroscopic features and stratigraphic context. Samples were collected as representative of different types of masonry in the aqueduct. Particularly, mortars were taken either between bricks (*opus latericium*), between stone blocks (*opus reticulatum*) or hydraulic plaster, from the internal duct along a 1-km-long tract of the aqueduct. Samples were collected by the aid of a hammer and chisel, at different heights to be representative of different environmental conditions (above or below water level, or on the vaults) (Supplementary data SUP1-2).

Preliminary analysis on the same samples by a multi-analytical approach including OM in thin sections, XRPD, SEM-EDS, and electron microprobe analysis (EMPA) [24] revealed that the mortar aggregate is mainly composed of pyroclastic products with pozzolanic behaviour from the Roman Magmatic Province. In particular, the results revealed that the aggregate is similar among the studied samples and it is of volcanic origin, with shapes ranging from rounded to sub-rounded and variable grain size. The volcanic materials with pozzolanic behaviour are pumice clasts, tuff, lava fragments, and pozzolan compatible with Vitruvius' *harena fossicia*. Artificial aggregate, such as crushed ceramic fragments, which are typical of a type of mortar called *cocciopesto*, has been found only in papal mortars. The binder in the Trajan samples is amorphous while the papal ones have a typical calcitic lime binder. The binder/aggregate ratio of Trajan Age samples was estimated to be about 1:3, and 1:2 in the papal samples [24].

2.2. Analytical techniques

2.2.1. Minero-petrographic analysis

Thin sections of each sample were analysed by polarized optical microscopy (OM) using a Zeiss D-7082 Oberkochen, and characterised according to Pecchioni's criteria [37]. Samples were analysed under both plane-polarised light (PPL) and cross-polarized light (XPL).

2.2.2. X-ray diffraction

A manual separation with the aid of a stereomicroscope was performed to collect only the binder fraction, which was then finely ground in agate mortar for X-ray Powder Diffraction measurements (XRPD). All samples were analysed using a Bruker D8 focus diffractometer with CuKα radiation, operating at 40 kV and 30 mA. The following instrumental parameters were chosen: 3–60° 2θ range, angular step of 0.02°/2θ, and 2 s counting time. Data processing, including semi-quantitative analysis based on the "Reference Intensity Ratio Method", was performed using XPowderX software [38].

2.2.3. Scanning Electron Microscopy

Representative thin sections were metalized with graphite and Scanning Electron Microscopy with Energy-Dispersive Spectroscopy (SEM-EDS) was carried out using a FEI Quanta 400, equipped with an EDS detector for microanalysis, to reveal the morphology and the elemental composition of the binder samples.

In addition, High Resolution Field Emission Scanning Electron Microscopy (HR-FESEM) and EDS microanalysis was performed using an AURIGA Zeiss Microscope (SNN-lab at Center for Nanotechnology for Engineering-CNIS, Sapienza University of Rome) equipped with a Bruker detector for EDS to characterise the binder at nanoscale.

2.2.4. Differential Scanning Calorimetry and Thermogravimetric Analysis

An SDT Q600 (TA Instruments) was used for simultaneous Differential Scanning Calorimetry and Thermogravimetric Analysis (DSC-TGA) measurements on the binder fraction, which was separated from the aggregate with the aid of a stereomicroscope. Powdered samples (average mass of ca. 10 mg) were placed in a platinum pan. An equilibrium temperature of 40 °C was maintained for 5 min, then the analysis was performed from 40 °C to 1000 °C with a heating rate of 20 °C/min. O_2 was used as purging gas at a rate of 100 mL/min.

2.2.5. Electron microprobe analysis

Electron Microprobe Analysis (EMPA) was carried out using a Cameca SX50 equipped with five wavelength-dispersive spectrometers and operated at 15 kV accelerating voltage, 15 nA beam current and 10

μm beam size. Element peaks and background were measured with counting times of 20 s and 10 s respectively. Reference standards and matrix corrections were applied as in [24].

2.2.6. Chemical attack with HCl

Representative Trajan samples were subjected to acid attack (5% diluted and concentrated HCl by dropping directly on the binder area) to reveal the presence of carbonates.

2.2.7. Fourier-Transform Infrared spectroscopy (FTIR)

After the separation with the aid of a stereomicroscope, the binder fraction of Trajan and papal samples was deposited onto a diamond compression cell and crushed to obtain a thin sample to be analysed in transmission mode. In addition, μ-ATR analysis was performed directly on thin sections of both Trajan and papal samples.

IR analyses were performed using a Nicolet iS50 Analytical FTIR Spectrometer coupled with a Continuum IR microscope. Spectra were acquired in the 4000–400 cm^{-1} range, with a spectral resolution of 2 cm^{-1} and a signal/noise ratio of 42,000:1. Fourier transform was performed on the sum of 200 scans.

2.2.8. X-ray Absorption Near Edge Structure (XANES)

Selected mortar samples belonging to the Trajan age were analysed at the I-18 beamline at the Diamond light source (UK) in the form of thin sections.

XAS is informative of the local structure around a selected atomic species, which is indicated as the absorber atom (Ca, in our case). The spectral features reflect the type, number, and distance of the first few coordination shells around the absorber atom (up to 5–8 Å). One of the main advantages of XAS over XRPD is that it can also detect amorphous phases, or phases where the concentration of the absorber element is very low compared to the major elements (down to few ppm).

XAS spectra were acquired in fluorescence mode at the Ca K-absorption edge (~4039 eV) in the energy range 3843–4419 eV (energy step 0.3 eV), using a monochromator equipped with Si 111 crystals.

Because of the low signal-to-noise ratio, only the near-edge part of the spectra (called X-ray absorption near-edge structure, or XANES), which has a stronger signal, was considered. In this case, it is not possible to extract the structural parameters, and the speciation of the absorber atom (Ca) can only be inferred by comparison with the spectra of Ca-reference compounds, or by performing a linear combination fitting (LCF) using these latter to match the sample spectrum.

The following references were measured in transmission mode: vaterite, apatite, calcium chloride ($CaCl_2$), calcium hydroxide (portlandite, $Ca(OH)_2$), calcium acetate ($C_4H_6CaO_4$), and calcium sulfate ($CaSO_4{\cdot}2H_2O$). Additional references were kindly provided by Dr. Laurent Cormier (Institut de Minéralogie, de Physique des Matériaux et de Cosmochimie, France), and included: calcite ($CaCO_3$), grossular ($Ca_3Al_2Si_3O_{12}$), wollastonite ($CaSiO_3$), diopside ($CaMgSi_2O_6$), and anorthite ($CaAl_2Si_2O_8$). Details on the experimental setup used to acquire the additional references can be found in Cormier et al. [39]. The XANES spectra were calibrated, background-subtracted, and normalized using the Demeter software package [40], which was also used to perform Linear Combination Fits (see the Results section).

2.2.9. N_2 adsorption/desorption measurements

Specific surface area (BET method) and textural properties were determined by the adsorption/desorption of N_2 at 77 K using a Micromeritics 3Flex 3500 Analyzer (Norcross, GA, USA) after sample outgassing at 110 °C for 3.5 h via thermally-controlled heating mantles, up to a residual pressure lower than 0.8 Pa. Pore-size distribution was determined by the BJH method [41] from the adsorption isotherm. The total pore volume was obtained by the rule of Gurvitsch [42]. The uncertainty was ±2 $m^2\ g^{-1}$ for the specific surface area values, ±0.005 $cm^3\ g^{-1}$ for the total pore volume values and ±0.2 nm for the pore diameters. Due to the apparent inhomogeneity of the samples, measurements were performed on two different portions of material to test the reproducibility.

3. Results

3.1. Characterization of mortar binders of Trajan Age and papal restoration

Samples of Trajan Age are characterised by the presence of an amorphous gel-like cementitious matrix (Fig. 1a–c) with colours ranging from green to brown (PPL). The binder is rich in Si and Al as revealed by EDS (Fig. 2a). XRPD defined the binder as mainly composed by clinopyroxene and K-feldspars, plus minor amount of biotite and, in few cases, analcime, whereas calcite was not detected (SUP3).

XRPD analysis, carried out on the sole binder fraction of the Trajan samples, showed results similar to those from both binder and aggregate, probably because the fine grain size of the aggregate makes it difficult to be separated by hand [43] (SUP3).

On the contrary, a calcitic lime binder was identified in the samples related to the restoration works carried out under Pope Paulus V. Optical Microscopy showed a micritic texture with bright white to beige colour and high birefringence with dark coloured neo-formed phases at PPL (Fig. 1b–d). In this case, XRPD highlighted the presence of calcite in addition to the other mineral phases found in the Trajan samples (SUP4). Accordingly, chemical analysis showed high content of Ca and minor amount of Si and Al (Fig. 2b).

Mortar samples were analysed by simultaneous DSC-TGA to estimate the percentage of calcite and to ascertain its absence in the samples of Trajan Age.

In the original Trajan mortar samples (Fig. 3) two main endothermic reactions occurred: the first is the release of absorbed water (around 82 °C) that caused a weight loss of 6.2%, and the second one is the dehydration of hydraulic compounds at about 437 °C with a weight loss of 5.2% [33,43–48].

The total weight loss was scarce; indeed, the residue was 88.7% and the absence of calcite was confirmed. The lack of this phase in the Trajan samples was further confirmed by the chemical attack with HCl: no reaction was observed under the stereomicroscope.

The DSC-TGA plot of a papal sample (Fig. 4) shows the occurrence of three endothermic events: at 90 °C adsorbed water caused a weight loss of 4.8%; at about 438 °C the dehydration of hydraulic compounds took place; and finally, at 748 °C the decomposition of carbonate phases occurred with a weight loss of 13% [49]. After the analysis, the residue (77.9%) was lower respect to the Trajan samples and the results allow estimating a 29.5% of calcite in the binder.

The CO_2/H_2O ratio (weight loss of carbonates >600 °C respect to the weight loss of hydraulic water in the 200–600 °C range) was calculated, in order to evaluate the hydraulic indices of the binder [50,51]. The results in Table 1 show higher hydraulic character for the Trajan Age mortars respect to the papal ones.

3.2. Detailed characterization of the gel-like amorphous binder

Micro-FTIR analysis performed on the powdered Trajan samples showed the presence of silicates (large absorption band at about 1000 cm^{-1} [52]) and some clay minerals by the absorption bands at about 3691 and 3623 cm^{-1} [53]. However, the contribution of clay minerals is not observed in FTIR spectra performed using μ-ATR on the sole binder fraction (Fig. 5).

Numerous EMP analyses were performed on the amorphous gel-like binder to better define its chemical composition; however, due to the amorphous nature of the binder, the analyses never reached the total of 100 wt% (maximum between 50 and 60 wt%). The results confirmed SEM-EDS data, showing a high content of SiO_2, followed by Al_2O_3; low content of CaO and K_2O. The comparison with reference data provided for Roman mortars from the Temple of Castor in Rome (117 BCE) [54]

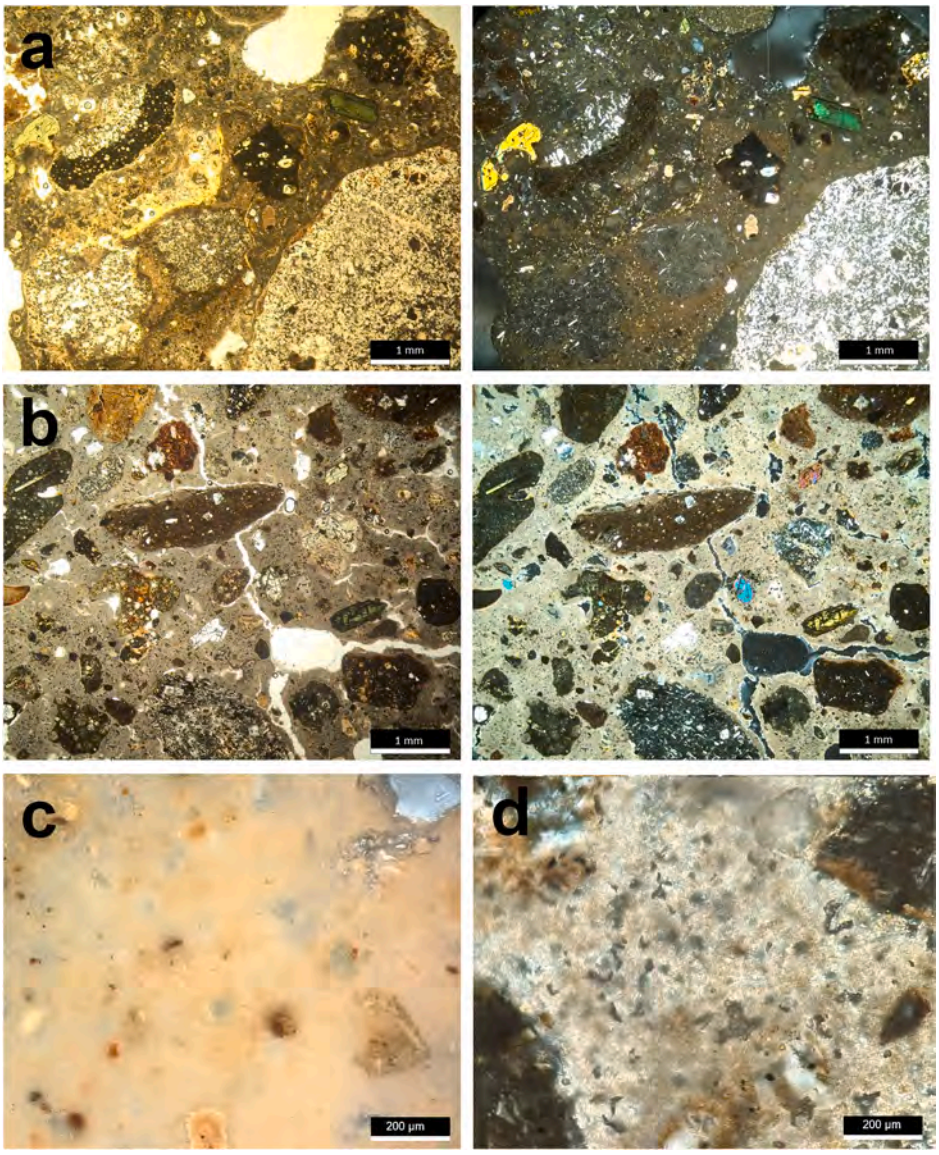

Fig. 1. OM micrographs showing (a) Trajan Age sample: the amorphous binder with an aggregate composed of fragments of volcanic rocks, pyroclastic rock fragments (red pozzolan) and crystals of feldspar, amphibole and pyroxene dispersed in the binder (sample TRA19, in PPL (left) and XPL (right)); (b) papal restoration sample: calcitic lime binder with micritic texture and aggregate of grog fragments mixed with porous pyroclastic rock fragments; amphiboles, pyroxene and feldspar are also dispersed in the binder (sample TRA34, in PPL (left) and XPL (right)); (c) Trajan Age sample: amorphous binder at higher magnification (sample TRA23 in XPL); (d) papal restoration sample: calcitic lime binder at higher magnification (sample TRA35 in XPL). (For interpretation of the references to colour in this figure legend, the reader is referred to the Web version of this article.)

highlights the peculiarity of the Trajan mortars, in which the amount of CaO is considerably lower than in literature data; consequently, an enrichment of Al_2O_3 and SiO_2 is observed.

Within fragments of pyroclastic products (tuff-type) with high porosity, pores filled with recrystallizations were identified. SEM images allowed to distinguished needle-shaped crystals from totally filled pores (Fig. 6). In the first case EMPA results indicated the presence of zeolites, chabazite type, whereas in the totally occluded pores the composition is similar to the amorphous binder, with a high content of Si and Al, scarce amounts of Ca, K, Na and Fe (Fig. 7).

Observations at higher magnification by HR-FESEM allowed to document needle-like formations dispersed in the binder matrix (Fig. 8). Chemical maps highlighted that the needle-like cementitious gel is mainly composed of Si, Al and Ca.

XAS spectra acquired at the Ca K-edge on the sole binder fraction were consistent (Fig. 9a), indicating a similar local structure around the Ca atom. Sample spectra were different from the relevant Ca-reference spectra (calcite, grossular, wollastonite, diopside, portlandite, anorthite, vaterite, apatite, Ca-sulfate, Ca-acetate, Ca-chloride, Fig. 9b), or from all their linear combinations, indicating that the above phases were not present. As the most common Ca-bearing crystalline phases did not reflect the Ca-speciation, to help reveal the Ca phases present in the samples, a range of aluminosilicate glasses with different Ca/Na and Si/Al ratios were obtained from Cormier and Neuville [39], where synthesis method and characterization of these soda lime aluminosilicate glasses can be found. As it can be seen in Fig. 9c, the spectral features of the mortar samples and of the aluminosilicate glasses are very similar. To try to improve the match, linear combinations using the aluminosilicate glasses were attempted using the set of synthetic silicate glasses reported in Table 2. The results show that the best fit with the spectra resulting from the average of all binder spectra can be obtained by combining roughly 54 ± 5 mol% of NCA30.30.00 and 46 ± 5 mol% of NCA60.00.20 (Fig. 9d).

This result indicates that the local structure around the Ca atoms is

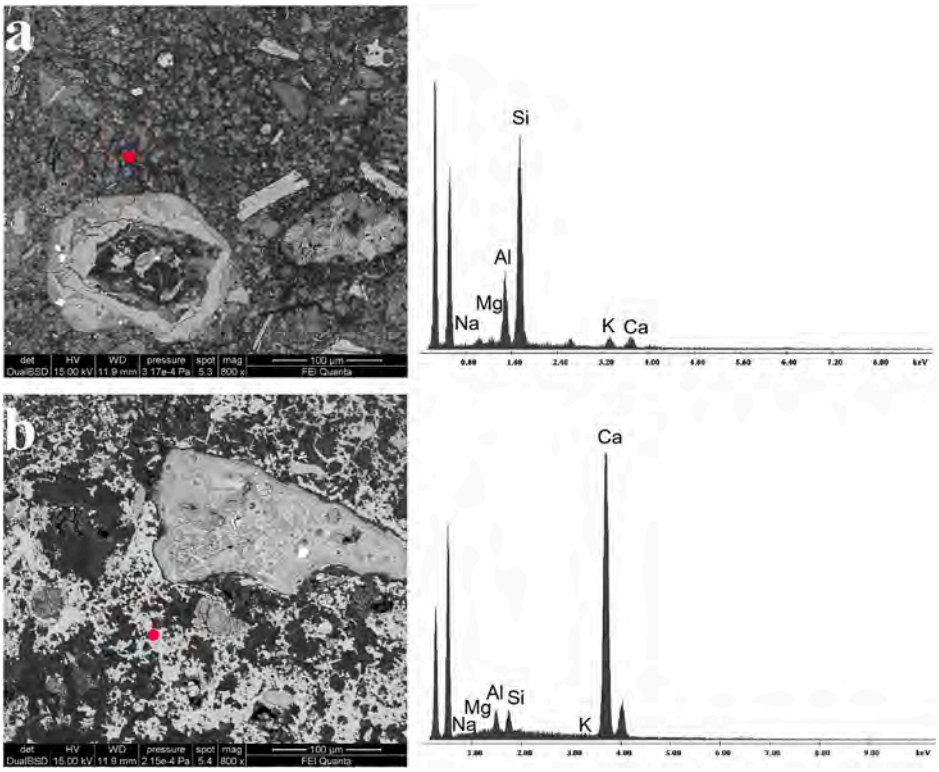

Fig. 2. SEM images (left) and EDS spectra (right) showing (a) Trajan Age sample: the amorphous gel-like binder (sample TRA11), and (b) papal restoration sample: the calcitic lime binder with micritic texture and neo-formed calcium aluminosilicate hydrate (white colour in BSE image) (sample TRA34). EDS spectra refer to the red dots in the SEM images. (For interpretation of the references to colour in this figure legend, the reader is referred to the Web version of this article.)

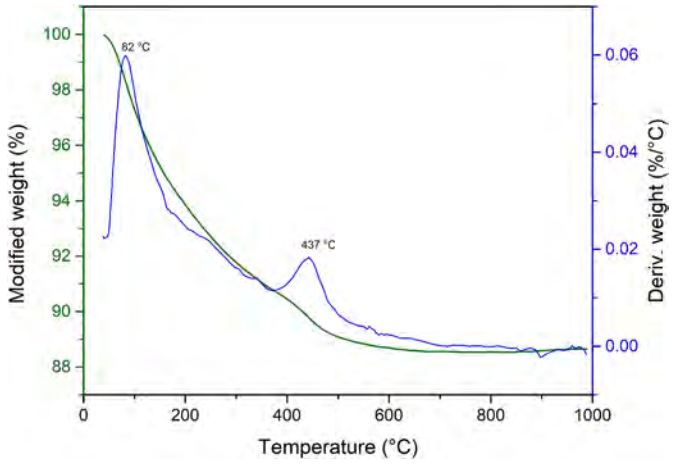

Fig. 3. TGA curve (green) and Derivative thermogravimetry (DTG) curve (blue) of a Trajan sample (TRA8). (For interpretation of the references to colour in this figure legend, the reader is referred to the Web version of this article.)

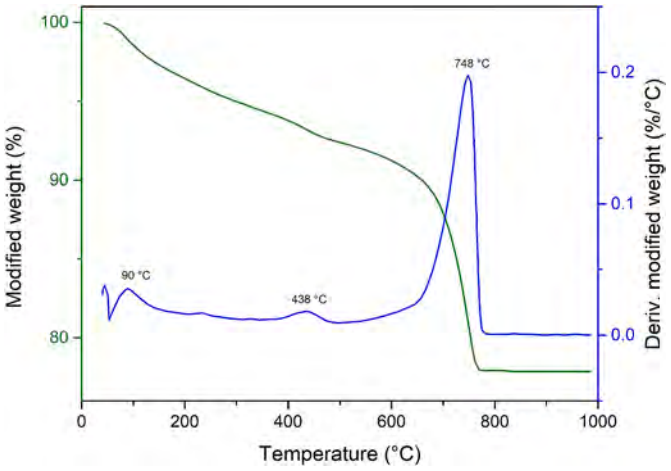

Fig. 4. TGA curve (green) and DTG curve (blue) of a papal sample (TRA35). (For interpretation of the references to colour in this figure legend, the reader is referred to the Web version of this article.)

similar to that of the aluminosilicate glasses. The minor mismatches with the sample spectra may be ascribed to the different Ca/Na and Si/Al ratios of the synthetic aluminosilicate glasses, which have a different chemical composition (Table 2) with respect to the mortar Trajan samples.

Overall, XAS data confirmed the absence of calcite, portlandite, and other crystalline Ca-bearing phases in the Trajan samples (at least at levels above ~5 mol%, which is the sensitivity of the LCF of XANES spectra) and indicated that an amorphous Ca-rich aluminosilicate phase (C-A-S-H) is the main Ca-bearing phase.

Finally, textural properties of the Trajan samples were analysed by nitrogen adsorption/desorption measurements. The results of specific surface area, total pore volume, and maximum values in the pore size distribution, are reported in Table 3.

These textural properties are typical for ancient Roman mortars,

Table 1
Calculation of CO_2/H_2O ratio from the TGA curve of Figs. 3 and 4.

Sample	Weight loss (wt. %) in each temperature range (°C)			CO_2/H_2O ratio
	<200	200–600	>600	
Trajan Age	6.2	5.2	0.1	0.02
papal	4.8	5.1	13	2.55

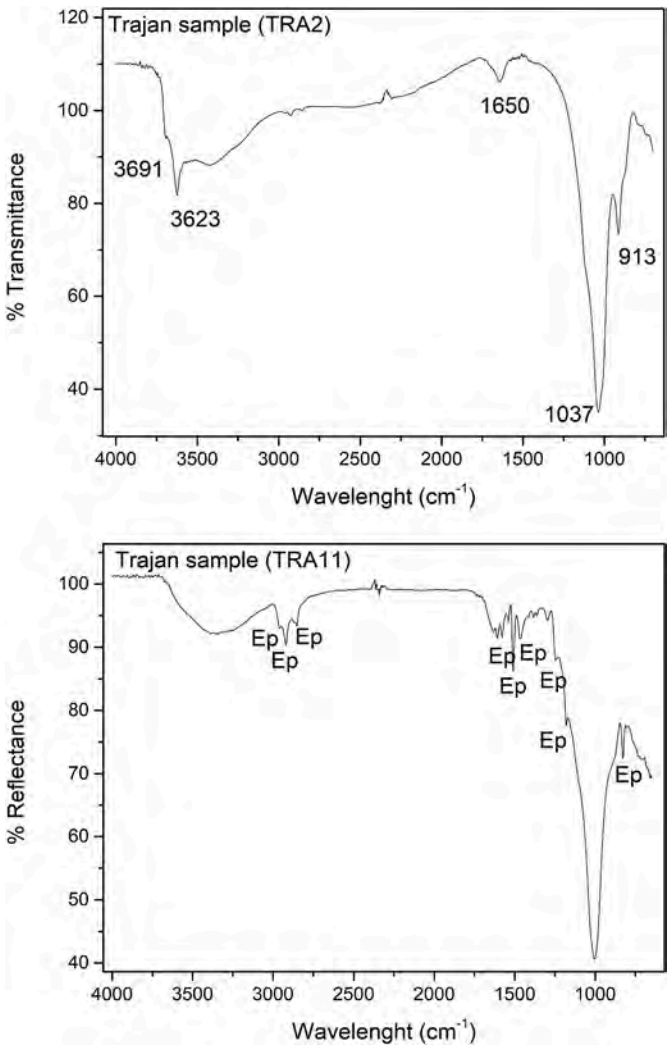

Fig. 5. Micro-FTIR spectrum of the powder Trajan sample (top sample TRA2) and μ-ATR spectrum of the binder fraction in thin section (bottom sample TRA11). The latter spectrum mainly shows the absorption bands of the embedding resin (Ep) of the thin section, and the band at about 1000 cm^{-1} related to silicate phases.

revealing the presence of mesopores with a small diameter (2–10 nm), generally much lower than pore sizes of modern hydraulic mortars, possibly affecting water adsorption and mechanical properties (high durability and resistance) of the mortars [29].

4. Discussion

All the mortar samples from the *Aqua Traiana* aqueduct can be defined as hydraulic mortars characterised by the presence of a pozzolanic aggregate [24]. It has been reported that the presence of pozzolan favours the hydraulic reaction [18] and therefore it is an important variable to take into account. Particularly, both the amorphous fraction in the pozzolan materials and the secondary alteration products in volcanic fragments (Fig. 6), i.e., the zeolites generated through the interaction with circulating water [55], strongly favour the hydraulicity [56]. However, we have to consider that the presence of analcime could be also due to the interaction with fluids during the setting and the concurrent alteration of typical zeolites (such as chabazite and phillipsite) in pyroclastic Italian deposits [57].

In addition to natural pozzolanic aggregate, artificial materials with pozzolanic behaviour were found only in the papal samples [24]. The use of ceramic fragments as aggregate in ancient Roman mortars is widely attested as an alternative or concomitant of pozzolan [37]; however, the reaction is not as strong as with pozzolan because of the lower $Ca(OH)_2$ consumption [58].

Therefore, the high durable resistance of ancient mortars [59] may be ascribed to hydraulic components with high percentage of amorphous fraction and zeolites.

Fig. 7. Bar diagram of EMPA results collected on gel-like matrix (top) and C-A-S-H filled pores (bottom).

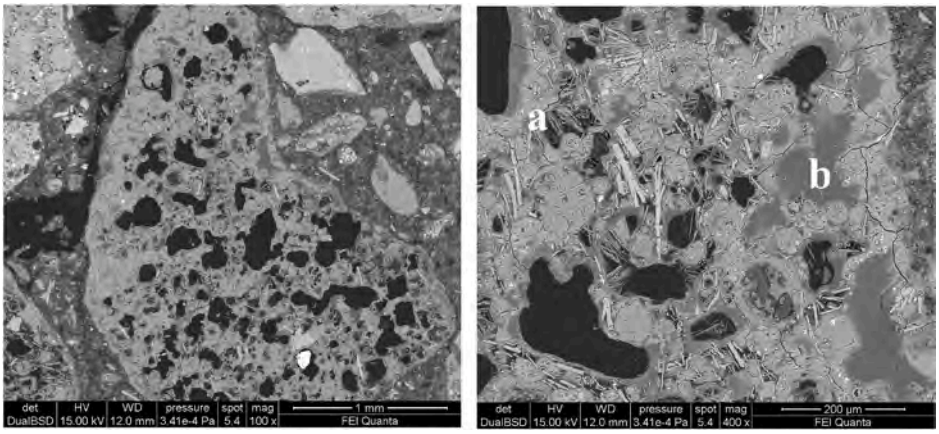

Fig. 6. SEM images of a pyroclastic product in a Trajan sample (TRA23): the magnified view highlights that vesicles contain (a) early C-A-S-H rims and later zeolite crystals and (b) C-A-S-H fillings.

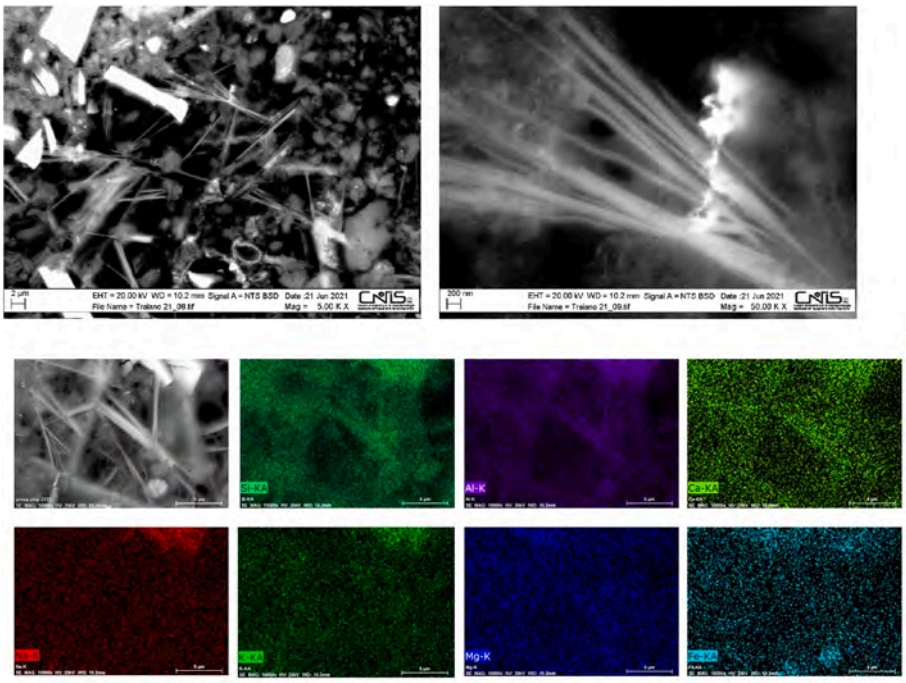

Fig. 8. FESEM images of a binder area in a Trajan sample (TRA21) at different magnifications showing a needle-like cementitious gel. A FESEM map shows that the needle-like formations in the binder are mainly composed of Si, Al and Ca.

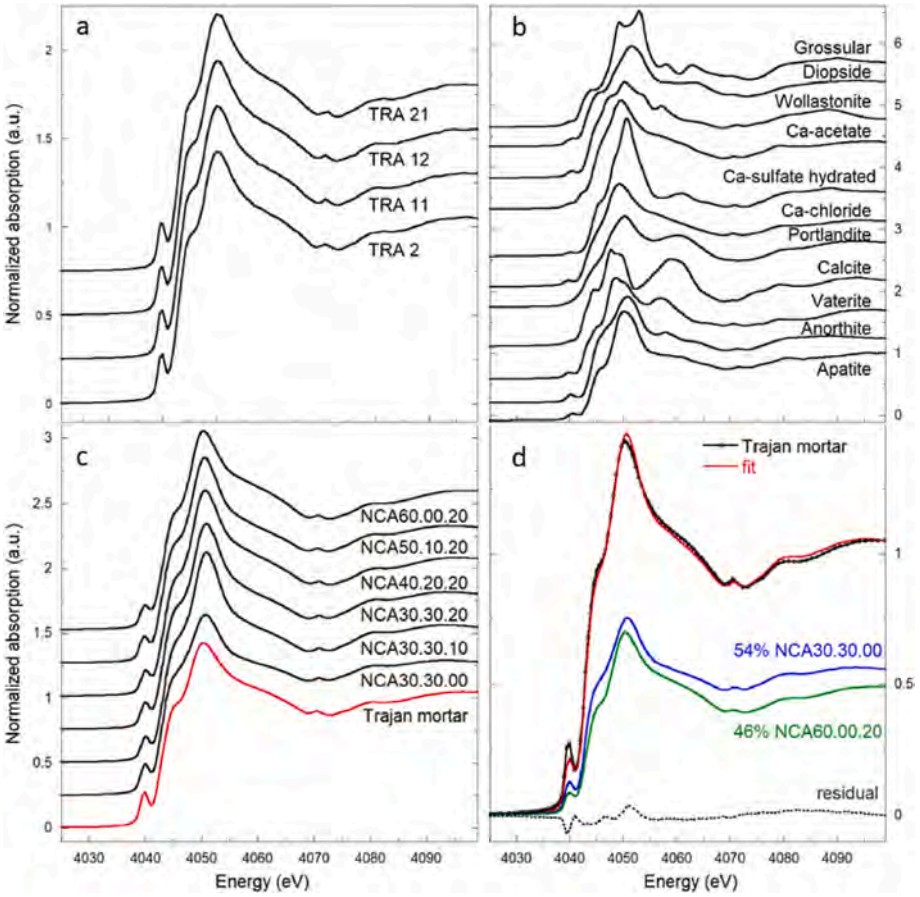

Fig. 9. a) XANES spectra of the Trajan mortar samples (TRA2, TRA11, TRA12, TRA21). b) XANES spectra of the crystalline Ca-references. c) XANES spectra of the Ca/Na-rich aluminosilicate glasses with different Ca/Na and Si/Al ratios from Cormier and Neuville [39] (Table 2), and of the average of the Trajan mortar spectra reported in panel (a). d) Best LCF of the Trajan mortar average spectrum using 54% of the NCA30.30.00 spectrum and 46% of the NCA60.00.20.

Table 2
Chemical composition (mol%) of the Ca/Na-rich aluminosilicate glasses (from Cormier and Neuville, 2004 [39]).

Glass sample	SiO_2 (mol%)	Al_2O_3 (mol%)	Na_2O (mol%)	CaO (mol%)
NCA60.00.20	60	0	20	20
NCA50.10.20	50	10	20	20
NCA40.20.20	40	20	20	20
NCA30.30.20	30	30	20	20
NCA30.30.10	30	30	10	30
NCA30.30.00	30	30	0	40

Table 3
BET specific surface area (S.A.), total pore volume (V_{tot}) and maximum values of pore diameter (D) of Trajan samples (TRA14, TRA19).

Sample	S.A. ($m^2 \cdot g^{-1}$)	V_{tot} ($cm^3 \cdot g^{-1}$)	D (nm)
TRA 14	51	0.138	2.0; 6.8
TRA 19	54	0.130	1.9; 7.3
TRA 14 (second test)	48	0.132	2.1; 7.4
TRA 19 (second test)	57	0.128	2.0; 6.2

The aggregate fraction is similar for papal and Trajan samples; conversely, the binder fraction constituted the main difference among them. Indeed, the results showed the presence of a calcitic lime binder in the samples related to the restoration of Pope Paulus V, whereas the samples of the Trajan Age are characterised by a calcite-free amorphous gel-like binder.

Air-hardening lime with the addition of natural and artificial materials with pozzolanic behaviour may explain the hydraulic characteristics of the papal samples [37]. Specifically, the hydraulic reaction of papal mortar might develop in three steps: 1) lime and water produce hydrated lime; 2) this latter is consumed by reactive silicates and aluminosilicates (from pozzolan and ceramic fragments), producing C–S–H and C-A-S-H; 3) calcite is formed by the reaction of CO_2 with unconsumed hydrated lime and/or as the result of the carbonatation of hydrated phases [4,54,56].

Amorphous gels, as the rim of pozzolanic aggregate, and calcite usually coexist and have been identified in other Roman architectures such as seawater harbours [5,14,60], the Trajan Markets [3], and a Roman cistern [46].

Hence, the absence of calcite in the original Trajan mortars from the *Aqua Traiana* is a unique case in archaeometric studies, and it could be due to different factors. For the aggregate, the abundant presence of materials with pozzolanic behaviour, and, particularly, glassy aggregates with limited amount of crystalline minerals, determines a high reactivity. Indeed, it is well known that amorphous structures are more reactive than the crystalline ones, due to the greater mobility of their atoms [56].

It is known that long-term pozzolanic reactions are controlled by many different variables, such as the content of silica and alumina [15], the chemical and mineralogical composition, the amount of active phases, the lime/pozzolan ratio, the water content, and the temperature [56]. The fine grain size of the aggregate in the Trajan mortars may facilitate a higher short-term pozzolanic reactivity [14,61] by increasing the specific area available for the chemical reaction with calcium hydroxide. The fine grain size also allows the pozzolanic reaction in the pores. Moropoulou et al. [62] observed that during hydraulic setting, lime penetrates into the fine aggregate reducing the pore size. On the contrary, with coarser aggregates the reaction does not develop very far into the pores of the aggregate, but it is limited to the surface, resulting in a better adhesion between binder and aggregate [63]. Nevertheless, it has to be considered that the specific surface area of the aggregates impacts on the water demand of the paste, whereas the amount of amorphous fraction determines the strength of the mortar [56].

Although very unlikely, another possibility could be the presence of reactive aggregates. It has been found that in some mortars the low amount of pozzolan and clay minerals could not explain high hydraulicity features [64]. Indeed, under specific conditions, plagioclase, feldspars, and other minerals can be destabilized releasing silicates and increasing the final hydraulicity. This results in reaction rims similar to those found around pozzolan inclusions [64], as can be observed on the border of the minerals dispersed into the Trajan binder [24]. This possibility has never been discussed in relation to historical mortars, but only for the alkali-silicate reaction (ASR) in Portland Cement concrete. However, it has been observed that in the presence of SiO_2 with lattice defects or low crystallinity, high humidity, high pH, and alkali content, this possibility should be taken into account [64].

Finally, the specific environmental conditions of the setting could have prevented carbonatation. In fact, the samples were collected inside a still-functioning aqueduct, where humidity is high and CO_2 scarce [12]. However, the sole environmental conditions cannot explain the difference among Trajan and papal samples, which were subjected to the same temperature and humidity conditions.

Considering the above discussion and the results of the analyses, the following reactions may have occurred in the original Trajan mortars: 1) marl mixed with water produced hydrated lime, 2) which was consumed by volcanic products enriched in alkali [65] producing a C-(N,K)-A-S-H gel with needle-like formations [4,54].

The low content of calcite in the starting raw material could have prevented portlandite carbonatation into calcite because all portlandite is consumed in the formation of C-A-S-H gels.

The CO_2/H_2O ratio calculated from DSC-TGA clearly indicates a high discrepancy in hydraulicity between the Trajan Age and papal samples, suggesting that the amorphous binder is the cause of the increased hydraulic characteristics of the Trajan mortars [43,50,66]. In addition, it was proved that the C-(N,K)-A-S-H gel is also responsible for the mechanical strength of the binder, similar to modern cement-based materials [14], as this silica gels form a fairly porous structure that is chemically stable and not subjected to volume expansion [64]. Textural analyses show the presence of finer pores than those in modern hydraulic mortars (up to 100 nm). It is possible to hypothesize that, by filling pores and favouring adhesion among aggregates, the gel improves the resistance to external agents (such as water in the aqueduct), and consequently the durability of the mortar [67].

5. Future benefit estimation

It is assumed that one chilogram of Portland clinker releases 0.87 Kg of CO_2 into the atmosphere [68]. In this way, the European annual carbon dioxide emissions due to the production of Portland clinker contribute to at least 8% of global CO_2 emissions [69]. It is generally agreed that such emissions should be decreased as required by Kyoto commitments. In addition, conservators need to repair deteriorated mortars and damaged masonries of historical buildings with mortars compatible with the original materials, and they strongly disagree with the employment of Portland cement for this task [59,70–72]. Therefore, the production of a material that could replace Portland cement with comparable or better mechanical features and lower CO_2 emissions would represent a landmark for modern building industry.

The addition of reactive aggregates (such as ash, slag, and volcanic pozzolan) as well as the use of clayey materials, has been proved to produce concretes with high workability, strength, and durability, that can also be more environmentally sustainable [68]. In particular, the addition of fine aggregates derived from waste material from other productions, can strongly improve the compression strength of mortars, due to a micro-filler effect [73].

The results of this work show that the raw materials used for the *Aqua Traiana* aqueduct may be a good choice in terms of strength and durability. In addition, the diffuse presence of amorphous hydraulic formations, as those identified in ancient mortars from aqueducts, determines a greater energy absorption, resulting in a higher resistance to continuous stress and strain [74].

Recent studies on geopolymers focused the attention on the materials and the alkaline activation, which could represent an alternative to cement production. In these studies, the product obtained by the main reaction, *i.e.* an amorphous aluminosilicate gel with small amount of zeolites [75], is similar to what identified in the ancient mortars studied in this work, suggesting that past recipes could be used as a guide to develop better and more sustainable cements.

6. Conclusions

This work analysed in detail the binder of mortar samples from the *Aqua Traiana* aqueduct to understand if it was the cause of the extraordinary resistance and durability of this monument. A mineralogical and chemical characterization of the original Trajan mortar binders, and those of papal restoration, was performed. Despite both binders containing similar aggregate, the papal samples are characterised by a calcitic lime binder, whereas the Trajan Age samples are characterised by an amorphous gel-like binder without calcite. The lack of calcite, in particular, has never been observed before in ancient binders.

The higher hydraulicity of the Trajan Age mortars suggests that the presence of an amorphous binder with needle-like shape results in enhanced hydraulic characteristics and improved mechanical strength. Therefore, the results indicate that the durability of the monument may be related to a calcite-free amorphous gel-like binder.

In addition, other parameters play an important role in determining the strength of mortars from the *Aqua Traiana*:

- the pozzolanic aggregate with variable grain size, high percentage of amorphous fraction, and high amounts of zeolites,
- the sole presence of natural materials providing pozzolanic behaviour (absence of artificial ones),
- the optimal binder/aggregate ratio,
- the diffuse presence of micro-pores instead of macro-ones.

However, despite the thorough characterization of the mortars of the *Aqua Traiana* aqueduct, a certain identification of which variable contributes the most to the final product has not been possible yet. New samples must be prepared and analysed to fully identify the recipe of the ancient mortars. In addition, the production steps required to obtain the C-(N,K)-A-S-H gel are still undefined, and further research is necessary.

The strength and durability observed in these ancient mortars offers an excellent model to produce improved mortars for modern applications, such as conservation and sustainable building. The lesson that can be learned from the past may lead to mortar binders with increased environmental sustainability, compatibility with original materials (in restoration), and high resistance to continuous stress and strain.

CRediT authorship contribution statement

Laura Medeghini: Conceptualization, Formal analysis, Funding acquisition, Investigation, Resources, Supervision, Writing – original draft. **Laura Calzolari:** Data curation, Investigation, Writing – original draft. **Michela Botticelli:** Data curation, Investigation, Writing – original draft. **Melania Di Fazio:** Formal analysis, Writing – review & editing. **Caterina De Vito:** Formal analysis, Writing – review & editing. **Ida Pettiti:** Data curation, Investigation, Writing – original draft. **Fabrizio Bardelli:** Data curation, Investigation, Writing – original draft. **Silvano Mignardi:** Funding acquisition, Investigation, Writing – original draft.

Declaration of competing interest

The authors of this manuscript declare that they have no conflict of interest.

Data availability

Data will be made available on request.

Acknowledgments

Financial support was provided by Sapienza University of Rome (Grant Medeghini Medi 2018) and by Distretto Tecnologico Beni e Attività Culturali – DTC Lazio and Lazio Innova DTC ON-TECH CUP F85F21001090003.

The authors thank the *Sovrintendenza Capitolina ai Beni Culturali*, Dr. F.M. Cifarelli and Dr. M. Marcelli, *Roma Sotterranea* speleological association, E. Santucci, *ACEA ATO 2*, Antonio Grosso and Armando Zitelli; and finally, Dr. G. Sidoti of the *Istituto Centrale del Restauro* for Thermogravimetric Analysis. We are grateful to Dr. Laurent Cormier for kindly providing some relevant Ca references and the synthetic Ca/Na-rich aluminosilicate glasses.

Appendix A. Supplementary data

Supplementary data to this article can be found online at https://doi.org/10.1016/j.cemconcomp.2024.105484.

References

[1] A. Moropoulou, A. Bakolas, S. Anagnostopoulou, Composite materials in ancient structures, Cem. Concr. Compos. 27 (2005) 295–300, https://doi.org/10.1016/j.cemconcomp.2004.02.018.

[2] L. Randazzo, M. Ricca, S. Ruffolo, M. Aquino, B. Petriaggi Davidde, F. Enei, M. La Russa, An integrated analytical approach to define the compositional and textural features of mortars used in the underwater archaeological site of Castrum, Minerals 9 (2019) 1–14.

[3] M.D. Jackson, J.M. Logan, B.E. Scheetz, D.M. Deocampo, C.G. Cawood, F. Marra, M. Vitti, L. Ungaro, Assessment of material characteristics of ancient concretes, Grande Aula, Markets of Trajan, Rome, J. Archaeol. Sci. 36 (2009) 2481–2492, https://doi.org/10.1016/j.jas.2009.07.011.

[4] M. Jackson, D. Deocampo, F. Marra, B. Scheetz, Mid-Pleistocene pozzolanic volcanic ash in ancient Roman concretes, Geoarchaeology 25 (2010) 36–74, https://doi.org/10.1002/gea.20295.

[5] M.D. Jackson, S.R. Mulcahy, H. Chen, Y. Li, Q. Li, P. Cappelletti, H.R. Wenk, Phillipsite and Al-tobermorite mineral cements produced through low-temperature water-rock reactions in Roman marine concrete, Am. Mineral. 102 (2017) 1435–1450, https://doi.org/10.2138/am-2017-5993CCBY.

[6] C.J. Brandon, R.L. Hohlfelder, M.D. Jackson, J.P. Oleson, Building for Eternity: the History and Technology of Roman Concrete Engineering in the Sea, Oxbow books, 2014.

[7] A. Palomo, P. Monteiro, P. Martauz, V. Bilek, A. Fernandez-Jimenez, Hybrid binders: A journey from the past to a sustainable future (*opus caementicium futurum*), Cement Concr. Res. 124 (2019) 105829, https://doi.org/10.1016/j.cemconres.2019.105829.

[8] F. Marra, D. Deocampo, M.D. Jackson, G. Ventura, The Alban Hills and Monti Sabatini volcanic products used in ancient Roman masonry (Italy): an integrated stratigraphic, archaeological, environmental and geochemical approach, Earth Sci. Rev. 108 (2011) 115–136, https://doi.org/10.1016/j.earscirev.2011.06.005.

[9] M. Jackson, F. Marra, Roman stone masonry: volcanic foundations of the ancient city, Am. J. Archaeol. 110 (2006) 403–436, https://doi.org/10.3764/aja.110.3.403.

[10] F. Marra, M. Anzidei, A. Benini, E. D'Ambrosio, M. Gaeta, G. Ventura, A. Cavallo, Petro-chemical features and source areas of volcanic aggregates used in ancient Roman maritime concretes, J. Volcanol. Geoth. Res. 328 (2016) 59–69, https://doi.org/10.1016/j.jvolgeores.2016.10.005.

[11] F. Marra, A. Danti, M. Gaeta, The volcanic aggregate of ancient Roman mortars from the Capitoline Hill: petrographic criteria for identification of Rome's "pozzolans" and historical implications, J. Volcanol. Geoth. Res. 308 (2015) 113–126, https://doi.org/10.1016/j.jvolgeores.2015.10.007.

[12] S. Sánchez-Moral, L. Luque, J.-C. Canaveras, V. Soler, J. Garcia-Guinea, A. Aparicio, Lime pozzolana mortars in Roman catacombs: composition, structures and restoration, Cement Concr. Res. 35 (2005) 1555–1565, https://doi.org/10.1016/j.cemconres.2004.08.009.

[13] M. Jackson, F. Marra, D. Deocampo, A. Vella, C. Kosso, R. Hay, Geological observations of excavated sand (*harenae fossiciae*) used as fine aggregate in Roman pozzolanic mortars, J. Rom. Archaeol. (2007) 25–53, https://doi.org/10.1017/s1047759400005304.

[14] G. Vola, E. Gotti, C. Brandon, J.P. Oleson, R.L. Hohlfelder, Chemical, mineralogical and petrographic characterization of Roman ancient hydraulic concretes cores from Santa Liberata, Italy, and Caesarea Palestinae, Israel, Period, Minerals 80 (2011) 317–338, https://doi.org/10.2451/2011PM0023.

[15] A. Tironi, M.A. Trezza, A.N. Scian, E.F. Irassar, Assessment of pozzolanic activity of different calcined clays, Cem. Concr. Compos. 37 (2013) 319–327, https://doi.org/10.1016/j.cemconcomp.2013.01.002.

[16] L. Kriskova, Y. Pontikes, Ö. Cizer, G. Mertens, W. Veulemans, D. Geysen, P. Tom, L. Vandewalle, K. Van Balen, B. Blanpain, Effect of mechanical activation on the hydraulic properties of stainless steel slags, Cement Concr. Res. 42 (2012) 778–788, https://doi.org/10.1016/j.cemconres.2012.02.016.

[17] L.M. Seymour, J. Maragh, P. Sabatini, M. Di Tommaso, J.C. Weaver, A. Masic, Hot mixing: mechanistic insights into the durability of ancient Roman concrete, Sci. Adv. 9 (2023) 1–13, https://doi.org/10.1126/sciadv.add1602.

[18] P. Maravelaki-Kalaitzaki, A. Galanos, I. Doganis, N. Kallithrakas-Kontos, Physico-chemical characterization of mortars as a tool in studying specific hydraulic components: application to the study of ancient Naxos aqueduct, Appl. Phys. A 104 (2011) 335–348, https://doi.org/10.1007/s00339-010-6143-9.

[19] M.O. Figueiredo, J.P. Veiga, T.P. Silva, Materials and reconstruction techniques at the Aqueduct of Carthage since the Roman period, Hist. Constr. Guimares. (2001) 391–400.

[20] G. Rizzo, L. Ercoli, B. Megna, M. Parlapiano, Characterization of mortars from ancient and traditional water supply systems in Sicily, J. Therm. Anal. Calorim. 92 (2008) 323–330, https://doi.org/10.1007/s10973-007-8758-4.

[21] Y. Benjelloun, J. de Sigoyer, J. Carlut, A. Hubert-Ferrari, H. Dessales, H. Pamir, V. Karabacak, Characterization of building materials from the aqueduct of Antioch-on-the-Orontes (Turkey), Compt. Rendus Geosci. 347 (2015) 170–180, https://doi.org/10.1016/j.crte.2014.12.002.

[22] L. Medeghini, V. Ferrini, F. Di Nanni, F.D. Uva, S. Mignardi, C. De Vito, Ceramic pipes of the Roman aqueduct from Raiano village (L'Aquila, Italy): a technological study, Construct. Build. Mater. 218 (2019) 618–627, https://doi.org/10.1016/j.conbuildmat.2019.05.137.

[23] L. Maritan, C. Mazzoli, R. Sassi, F. Speranza, A. Zanco, P. Zanovello, Trachyte from the Roman aqueducts of Padua and Este (north-east Italy): a provenance study based on petrography, chemistry and magnetic susceptibility, Eur. J. Mineral 25 (2013) 415–427, https://doi.org/10.1127/0935-1221/2013/0025-2282.

[24] M. Botticelli, L. Calzolari, C. De Vito, S. Mignardi, L. Medeghini, *Aqua Traiana*, a Roman infrastructure embedded in the present: the mineralogical perspective, Minerals 11 (2021), https://doi.org/10.3390/min11070703.

[25] L. Calzolari, C. Rea, C. De Vito, S. Mignardi, L. Medeghini, Lithic materials from the 109 AD Roman aqueduct *Aqua Traiana*, (Sette Botti caput aquae, Rome), Period. Mineral. 92 (2023).

[26] C. Genestar, C. Pons, A. Más, Analytical characterisation of ancient mortars from the archaeological Roman city of Pollentia (Balearic Islands, Spain), Anal. Chim. Acta 557 (2006) 373–379, https://doi.org/10.1016/j.aca.2005.10.058.

[27] L.M. Seymour, N. Tamura, M.D. Jackson, A. Masic, Reactive binder and aggregate interfacial zones in the mortar of Tomb of Caecilia Metella concrete, 1C BCE, Rome, J. Am. Ceram. Soc. 105 (2022) 1503–1518, https://doi.org/10.1111/jace.18133.

[28] S. Columbur, F. Sitzia, G. Ennas, The ancient pozzolanic mortars and concretes of *Heliocaminus* baths in Hadrian's Villa (Tivoli, Italy), Archaeol. Anthropol. Sci. 9 (2017) 523–553, https://doi.org/10.1007/s12520-016-0385-1.

[29] C. Rispoli, R. Esposito, L. Guerriero, P. Cappelletti, Ancient Roman mortars from Villa del Capo di Sorrento: a multi-analytical approach to define microstructural and compositional features, Minerals 11 (2021), https://doi.org/10.3390/min11050469.

[30] J. Hormes, Q. Xiao, Y. Hu, C. Bläuer, A. Diekamp, J. Goll, G.L. Bovenkamp, Mortar samples from the Abbey of Saint John at Müstair: a combined spatially resolved X-ray fluorescence and X-ray absorption (XANES) study, J. Anal. At. Spectrom. 30 (2015) 702–706, https://doi.org/10.1039/c4ja00401a.

[31] J. Hormes, A. Diekamp, W. Klysubun, G.L. Bovenkamp, N. Börste, The characterization of historic mortars: a comparison between powder diffraction and synchrotron radiation based X-ray absorption and X-ray fluorescence spectroscopy, Microchem. J. 125 (2016) 190–195, https://doi.org/10.1016/j.microc.2015.11.034.

[32] G. Ponce-Antón, M.C. Zuluaga, L.A. Ortega, J.A. Mauleon, Petrographic and chemical–mineralogical characterization of mortars from the cistern at Amaiur Castle (Navarre, Spain), Minerals 10 (2020) 1–16.

[33] J. Lanas, J.L.P. Bernal, M.A. Bello, J.I.A. Galindo, Mechanical properties of natural hydraulic lime-based mortars, Cement Concr. Res. 34 (2004) 2191–2201, https://doi.org/10.1016/j.cemconres.2004.02.005.

[34] E.J. Dembskey, The Aqueducts of Ancient Rome, University of South Africa, 2009.

[35] P. Pace, Acquedotti di Roma e il De Aquaeductu di Frontino, third ed., B&T Multimedia, 2010.

[36] T. Ashby, Gli Aquedotti Dell'antica Roma, Quasar, Roma, 1991.

[37] E. Pecchioni, F. Fratini, E. Cantisani, Atlas of the Ancient Mortars in Thin Section under Optical Microscope, Nardini, 2017.

[38] J. Martin, Using XPowder: A Software Package for Powder X-Ray Diffraction Analysis, D.L. GR 1001/04, Spain, 2004.

[39] L. Cormier, D.R. Neuville, Ca and Na environments in Na_2O-CaO-Al_2O_3-SiO_2 glasses: influence of cation mixing and cation-network interactions, Chem. Geol. 213 (2004) 103–113, https://doi.org/10.1016/j.chemgeo.2004.08.049.

[40] B. Ravel, M. Newville, ATHENA, artemis, hephaestus: data analysis for X-ray absorption spectroscopy using IFEFFIT, J. Synchrotron Radiat. 12 (2005) 537–541, https://doi.org/10.1107/S0909049505012719.

[41] E.P. Barrett, L.G. Joyner, P.P. Halenda, The determination of pore volume and area distributions in porous substances. I. Computations from nitrogen isotherms, J. Am. Chem. Soc. 73 (1951) 373–380.

[42] L. Gurvitsch, Physicochemical attractive force, J. Phys. Chem. Soc. Russ. 47 (1915) 805–827.

[43] J. Elsen, K. Van Balen, G. Mertens, Hydraulicity in historic lime mortars: a review, RILEM Bookseries 7 (2013) 125–139, https://doi.org/10.1007/978-94-007-4635-0_10.

[44] S. Thirumalini, R. Ravi, S.K. Sekar, M. Nambirajan, Knowing from the past - ingredients and technology of ancient mortar used in Vadakumnathan temple, Tirussur, Kerala, India, J. Build. Eng. 4 (2015) 101–112, https://doi.org/10.1016/j.jobe.2015.09.004.

[45] A. Moropoulou, A. Bakolas, K. Bisbikou, Characterization of ancient, byzantine and later historic mortars by thermal and X-ray diffraction techniques, Thermochim. Acta 269–270 (1995) 779–795, https://doi.org/10.1016/0040-6031(95)02571-5.

[46] D.A. Silva, H.R. Wenk, P.J.M. Monteiro, Comparative investigation of mortars from Roman Colosseum and cistern, Thermochim. Acta 438 (2005) 35–40, https://doi.org/10.1016/j.tca.2005.03.003.

[47] C. Rispoli, A. De Bonis, R. Esposito, S.F. Graziano, A. Langella, M. Mercurio, V. Morra, P. Cappelletti, Unveiling the secrets of Roman craftsmanship: mortars from *Piscina Mirabilis* (*Campi Flegrei*, Italy), Archaeol. Anthropol. Sci. 12 (2020) 1–18, https://doi.org/10.1007/s12520-019-00964-8.

[48] E. L'Hôpital, B. Lothenbach, K. Scrivener, D.A. Kulik, Alkali uptake in calcium alumina silicate hydrate (C-A-S-H), Cement Concr. Res. 85 (2016) 122–136, https://doi.org/10.1016/j.cemconres.2016.03.009.

[49] M.L. Santarelli, F. Sbardella, M. Zuena, J. Tirillò, F. Sarasini, Basalt fiber reinforced natural hydraulic lime mortars: A potential bio-based material for restoration, J. Mater. 63 (2014) 398–406, https://doi.org/10.1016/j.matdes.2014.06.041.

[50] A. Bakolas, G. Biscontin, A. Moropoulou, E. Zendri, Characterization of structural Byzantine mortars by thermogravimetric analysis, Thermochim. Acta 321 (1998) 151–160, https://doi.org/10.1016/s0040-6031(98)00454-7.

[51] G. Biscontin, M. Pellizon Birelli, E. Zendri, Characterization of binders employed in the manufacture of Venetian historical mortars, J. Cult. Herit. 3 (2002) 31–37, https://doi.org/10.1016/S1296-2074(02)01156-1.

[52] C. Miliani, F. Rosi, A. Daveri, B.G. Brunetti, Reflection infrared spectroscopy for the non-invasive in situ study of artists' pigments, Appl. Phys. Mater. Sci. Process 106 (2012) 295–307, https://doi.org/10.1007/s00339-011-6708-2.

[53] J. Madejová, FTIR techniques in clay mineral studies, Vib. Spectrosc. 31 (2003) 1–10, https://doi.org/10.1016/S0924-2031(02)00065-6.

[54] D.M. Roy, C.A. Langton, Studies of Ancient Concrete as Analogs of Cementitious Sealing Materials for a Repository in Tuff, Los Alamos, NM (United States), 1989, https://doi.org/10.2172/60684.

[55] P. Cappelletti, A. Langella, A. Colella, R. De Gennaro, Mineralogical and technical features of zeolite deposits from northern Latium volcanic district, Period Mineral 68 (1999) 127–144.

[56] R. Walker, S. Pavia, Physical properties and reactivity of pozzolans, and their influence on the properties of lime–pozzolan pastes, Mater. Struct. 44 (2011) 1139–1150, https://doi.org/10.1617/s11527-010-9689-2.

[57] R.L. Hay, R.A. Sheppard, Occurrence of zeolites in sedimentary rocks: An overview, 45, Rev. Mineral. Geochem. 45 (1) (2001) 217–234, 217–234.

[58] A. Moropoulou, A. Bakolas, E. Aggelakopoulou, Evaluation of pozzolanic activity of natural and artificial pozzolans by thermal analysis, Thermochim. Acta 420 (2004) 135–140, https://doi.org/10.1016/j.tca.2003.11.059.

[59] G. Baronio, L. Binda, Study of the pozzolanicity of some bricks and clays, Construct. Build. Mater. 11 (1997) 41–46.

[60] M.D. Jackson, S.R. Chae, S.R. Mulcahy, C. Meral, R. Taylor, P. Li, A. Emwas, J. Moon, S. Yoon, G. Vola, H. Wenk, P.J.M. Monteiro, Unlocking the secrets of Al-tobermorite in Roman seawater concrete, Am. Mineral. 98 (2013) 1669–1687, https://doi.org/10.2138/am.2013.4484.

[61] Y. Zhao, J. Gao, C. Liu, X. Chen, Z. Xu, The particle-size effect of waste clay brick powder on its pozzolanic activity and properties of blended cement, J. Clean. Prod. 242 (2020) 118521, https://doi.org/10.1016/j.jclepro.2019.118521.

[62] A. Moropoulou, A. Bakolas, K. Bisbikou, Investigation of the technology of historic mortars, J. Cult. Herit. 1 (2000) 45–58.

[63] J. Nežerka, J. Němeček, Z. Slížková, P. Tesárek, Investigation of crushed brick-matrix interface in lime-based ancient mortar by microscopy and nanoindentation, Cem. Concr. Compos. 55 (2015) 122–128, https://doi.org/10.1016/j.cemconcomp.2014.07.023.

[64] J. Weber, A. Baragona, F. Pintér, C. Gosselin, Hydraulicity in ancient mortars: its origin and alteration phenomena under the microscope, 15th Euroseminar Microsc, Appl. to Build. Mater. (2015) 147–156.

[65] B. Giaccio, I. Arienzo, G. Sottili, F. Castorina, M. Gaeta, S. Nomade, P. Galli, P. Messina, Isotopic (Sr-Nd) and major element fingerprinting of distal tephras: an application to the Middle-Late Pleistocene markers from the Colli Albani volcano, central Italy, Quat. Sci. Rev. 67 (2013) 190–206, https://doi.org/10.1016/j.quascirev.2013.01.028.

[66] P. Maravelaki-Kalaitzaki, A. Bakolas, A. Moropoulou, Physico-chemical study of Cretan ancient mortars, Cement Concr. Res. 33 (2003) 651–661, https://doi.org/10.1016/S0008-8846(02)01030-X.

[67] C. Rispoli, A. De Bonis, V. Guarino, S.F. Graziano, C. Di Benedetto, R. Esposito, V. Morra, P. Cappelletti, The ancient *pozzolanic* mortars of the Thermal complex of Baia (*Campi Flegrei*, Italy), J. Cult. Herit. 40 (2019) 143–154, https://doi.org/10.1016/j.culher.2019.05.010.

[68] K. Celik, M.D. Jackson, M. Mancio, C. Meral, A. Emwas, P.K. Mehta, P.J.M. Monteiro, High-volume natural volcanic pozzolan and limestone powder as partial replacements for portland cement in self-compacting and sustainable concrete, Cem. Concr. Compos. 45 (2014) 136–147, https://doi.org/10.1016/j.cemconcomp.2013.09.003.

[69] R.M. Andrew, Global CO_2 emissions from cement production, Earth Syst. Sci. Data 10 (2018) 195–217, https://doi.org/10.5194/essd-10-195-2018.

[70] P. Degryse, J. Elsen, M. Waelkens, Study of ancient mortars from Sagalassos (Turkey) in view of their conservation, Cem. Concr. Compos. 32 (2002) 1457–1463.
[71] A. Güleç, T. Tulun, Physico-chemical and petrographical studies of old mortars and plasters of Anatolia, Cement Concr. Res. 27 (1997) 227–234.
[72] O. Cazalla, E. Sebastián, G. Cultrone, M. Nechar, M.G. Bagur, Three-way ANOVA interaction analysis and ultrasonic testing to evaluate air lime mortars used in cultural heritage conservation projects, Cement Concr. Res. 29 (1999) 1749–1752.
[73] J. Silva, J. de Brito, R. Veiga, Incorporation of fine ceramics in mortars, Construct. Build. Mater. 23 (2009) 556–564, https://doi.org/10.1016/j.conbuildmat.2007.10.014.
[74] A. Moropoulou, A.S. Cakmak, G. Biscontin, A. Bakolas, E. Zendri, Advanced Byzantine cement based composites resisting earthquake stresses: the crushed brick lime mortars of Justinian's Hagia Sophia, Construct. Build. Mater. 16 (2002) 543–552.
[75] A. Palomo, G. Fernàndez-Jiménez, A. Kovalchuk, L.M. Ordeñez, M.C. Naranjo, Opc-fly ash cementitious systems: study of gel binders produced during alkaline hydration, J. Mater. Sci. 42 (2007) 2958–2966, https://doi.org/10.1007/s10853-006-0585-7.